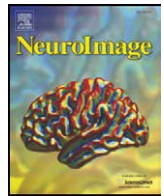




Contents lists available at ScienceDirect

NeuroImage

journal homepage: www.elsevier.com/locate/ynimg

White matter abnormalities revealed by diffusion tensor imaging in non-demented and demented HIV+ patients

Yasheng Chen ^{a,*}, Hongyu An ^a, Hongtu Zhu ^b, Taylor Stone ^a, J. Keith Smith ^a, Colin Hall ^c, Elizabeth Bullitt ^d, Dinggang Shen ^a, Weili Lin ^a

^a Department of Radiology, University of North Carolina School of Medicine, Chapel Hill, NC, USA

^b Department of Biostatistics, University of North Carolina at Chapel Hill, Chapel Hill, NC, USA

^c Department of Neurology, University of North Carolina School of Medicine, Chapel Hill, NC, USA

^d Department of Surgery, University of North Carolina School of Medicine, Chapel Hill, NC, USA

ARTICLE INFO

Article history:

Received 29 January 2009

Revised 4 March 2009

Accepted 4 April 2009

Available online xxx

ABSTRACT

HIV associated dementia (HAD) is the most advanced stage of central nervous system disease caused by HIV infection. Previous studies have demonstrated that patients with HAD exhibit greater cerebral and basal ganglia atrophy than non-demented HIV+ (HND) patients. However, the extent to which white matter is affected in HAD patients compared to HND patients remains elusive. This study is designed to address the potential white matter abnormalities through the utilization of diffusion tensor imaging (DTI) in both HND and HAD patients. DTI and T1-weighted images were acquired from 18 healthy controls, 21 HND and 8 HAD patients. T1 image-based registration was performed to 1) parcellate the whole brain white matter into major white matter regions, including frontal, parietal, temporal and occipital white matter, corpus callosum and internal capsule for statistical comparisons of the mean DTI values, and 2) warp all DTI parametric images towards the common template space for voxel-based analysis. The statistical comparisons were performed with four DTI parameters including fractional anisotropy (FA), mean (MD), axial (AD), and radial (RD) diffusivities. With Whitney U tests on the mean DTI values, both HND and HAD demonstrated significant differences from the healthy control in multiple white matter regions. In addition, HAD patients exhibited significantly elevated MD and RD in the parietal white matter when compared to HND patients. In the voxel-based analysis, widespread abnormal regions were identified for both HND and HAD patients, although a much larger abnormal volume was observed in HAD patients for all four DTI parameters. Furthermore, both region of interest (ROI) based and voxel-based analyses revealed that RD was affected to a much greater extent than AD by HIV infection, which may suggest that demyelination is the prominent disease progression in white matter.

© 2009 Elsevier Inc. All rights reserved.

Introduction

HIV+ patients in the most advanced stage may develop dementia, also known as the AIDS Dementia Complex, or HIV Associated Dementia (HAD) (McArthur et al., 1993). HAD has been shown to occur in 20% to 30% of untreated adult patients (Albright et al., 2003). The clinical symptoms of HAD include disabling cognitive impairment accompanied by motor dysfunction or change in behavior (or both) (AIDSTaskForce, 1991). Although to a large extent the pathogenesis of HAD or cognitive impairment caused by HIV infection remains unknown, brain macrophages and microglial cells are likely to be the key infected cells and responsible in the pathogenesis of HIV-associated neurocognitive impairment (Gonzalez-Scarano and Mar-

tin-Garcia, 2005). It is believed that the activation of these macrophages and/or microglial cells, along with a release of inflammatory cytokines and chemokines, leads to abnormal neuronal pruning (Moroni and Antinori, 2003). The most common histopathological findings in autopsy studies of AIDS patients suffering from dementia include: white matter changes and demyelination, microglial nodules, multinucleated giant cells, and perivascular infiltrate (Gray et al., 2003; Langford et al., 2003; Masliah et al., 2000). Furthermore, immunohistological studies also demonstrated that axonal injury occurs in both earlier and advanced stages of the disease (An and Scaravilli, 1997; Giometto et al., 1997; Gray et al., 1998; Medana and Esiri, 2003; Raja et al., 1997).

DTI is a superb white matter imaging modality capable of non-invasively revealing physiological parameters related to water diffusion in the brain (Basser et al., 1994). Due to the presence of myelin sheaths and microstructural components of axons in white matter, water molecules move more freely along than perpendicularly to the long axis of the fiber. This phenomenon is known as anisotropic

* Corresponding author. Dept. of Radiology, Campus Box 7515, University of North Carolina at Chapel Hill, Chapel Hill, NC 27599. Tel.: +1 919 843 4139; fax: +1 919 843 4456.

E-mail address: yasheng_chen@med.unc.edu (Y. Chen).

diffusion. Disruption of white matter structural integrity may alter both the magnitude and the anisotropy of water diffusion. As a result, changes in DTI parameters including fractional anisotropy (FA), mean diffusivity (MD), axial diffusivity (AD), and radial diffusivity (RD) may reflect microstructural abnormality of white matter.

FA and apparent diffusion coefficient (ADC, equivalent to MD) have been utilized to explore neurological dysfunction resulting from HIV infection (Cloak et al., 2004; Filippi et al., 2001; Pomara et al., 2001; Ragin et al., 2004a; Ragin et al., 2004b; Ragin et al., 2005; Thurnher et al., 2005). Filippi et al. (2001) found a correlation between the viral load and reduction of FA in the splenium and genu of the corpus callosum in 10 HIV infected subjects. Pomara et al. (2001) reported that FA decreased in white matter of the frontal lobes and increased in the posterior limb of the internal capsule in a cohort of 6 non-demented HIV+ patients when compared to 9 age-matched normal volunteers, but found no group difference in ADC, proton density, or T2-weighted images. Using whole-brain DTI histogram analysis, Ragin et al. (2004b) demonstrated that a reduction of the mean FA was significantly associated with the severity of dementia, while there was no significant correlation between elevated ADC and the clinical stage. In addition, they found that DTI measures in the sub-cortical regions were significantly correlated with a loss of function in specific cognitive domains (Ragin et al., 2004a; Ragin et al., 2005). Cloak et al. (2004) showed increased frontal white matter ADC in association with increased glial metabolites in 11 HIV infected subjects when compared to 14 seronegative subjects. ADC was correlated positively with the glial marker myoinositol and negatively with psychomotor efficiency, suggesting that the increased brain water diffusion may reflect increased glial activation or inflammation. With regions of interest (ROIs) placed in the splenium and genu of the corpus callosum, frontal white matter, and hippocampus in patients grouped with the viral loads and CD4 counts, Thurnher et al. (2005) reported significantly reduced FA and increased ADC only in genu of HIV+ patients and no statistically significant correlation existed between FA (and ADC) values and CD4 counts. More recently, voxel-based DTI analysis using Statistical Parametric Mapping (SPM) has demonstrated significantly increased MD in the seropositive population when compared to seronegative subjects (Stebbins et al., 2007).

While these reported findings clearly demonstrate the potential clinical utility of DTI in discerning white matter abnormalities resulting from HIV viral infection, most of the studies to date have only focused on comparing HIV+ patients with healthy controls. Relatively little effort has been given to examine how white matter abnormalities may be associated with different cognitive impairment levels in HIV+ populations. In addition, both white matter demyelination and axonal damage have been reported in HIV+ patients (An and Scaravilli, 1997; Giometto et al., 1997; Gray et al., 1998; Medana and Esiri, 2003; Raja et al., 1997; Price et al., 1988; Raja et al., 1997; Gray et al., 1996; Liuzzi et al., 1992). However, both FA and ADC (or MD) have been considered as non-specific markers because they are affected by many white matter characteristics such as myelination, axonal density, and integrity (Kraus et al., 2007; Song et al., 2002; Sun et al., 2006). Conversely, it has been suggested that axial and radial diffusivities may reflect axonal injury and demyelination, respectively (Song et al., 2002; Sun et al., 2006). Separate analyses of the changes in these two diffusivities may potentially provide more insights into the underlying mechanisms of white matter injury caused by HIV infection.

In this study, we specifically focused on the following three areas. *First*, we evaluated white matter abnormalities using two different approaches: ROI-based comparisons by parcellating whole brain white matter into different ROIs and voxel-based comparisons, allowing a more comprehensive analysis of white matter abnormality caused by HIV infection. *Second*, we determined white matter abnormalities present in HND and HAD patients separately, since white matter abnormalities may be different in HND and HAD patients. In addition, separating HND and HAD patients also allowed us to address whether

DTI can discern HAD from HND. *Third*, we extended the statistical comparisons to both axial and radial diffusivities instead of only analyzing FA and MD, allowing, potentially, to determine the relative severity of myelin loss and axonal damage in both HND and HAD.

Materials and methods

Patients

This study was approved by the Office of Human Research Ethics at our institution. Written informed consent was obtained from all subjects. In total, twenty-nine HIV+ patients (age ranged 41.2 ± 7.4 , 21 M and 8F) and eighteen age-matched healthy controls (age ranged 40.3 ± 5.6 , 9M and 9F) were studied. Patients were further divided into HND (age ranged 30.9 ± 7.7 , 17M and 4F) and HAD (age ranged 44.8 ± 5.8 , 4M and 4F) groups. The diagnosis of HAD was made in accordance with the criteria recommended by the American Academy of Neurology AIDS Task Force (1991). Of the 29 HIV+ patients, eighteen patients (13 in HND and 5 in HAD) received HAART. The viral loads in blood ranged from undetectable to $>65,000$.

MR imaging

All images were acquired using a 3T Allegra head only MR system (Siemens Medical Inc., Erlangen, Germany) with a maximal gradient strength of 40 mT/m and a maximal slew rate of 400 mT/(m ms). A standard circularly polarized head coil was used as the transmit/receive coil. High resolution T1 weighted images were acquired using a 3D MP-RAGE sequence with the imaging parameters as follows: TR/TE = 1700/4.38 ms, TI = 900 ms, field of view (FOV) = 256 mm² and an isotropic voxel size of $1 \times 1 \times 1$ mm³. A single shot EPI DTI sequence (TR/TE = 5400/73 ms) was used to obtain DTI images. Diffusion gradients with a *b*-value of 1000 s/mm² were applied in six non-collinear directions, $(1, 0, 1)/\sqrt{2}$, $(-1, 0, 1)/\sqrt{2}$, $(0, 1, 1)/\sqrt{2}$, $(0, 1, -1)/\sqrt{2}$, $(1, 1, 0)/\sqrt{2}$, and $(-1, 1, 0)/\sqrt{2}$. A reference scan (*b* = 0) was also obtained for diffusion tensor matrix calculation. Forty-six contiguous slices with a slice thickness of 2 mm covered a field of view of 256 mm with an isotropic voxel size $2 \times 2 \times 2$ mm³. Eighteen acquisitions were averaged to improve the signal-to-noise ratio (SNR) of the images. Four scalar DTI parameters, including FA, MD, AD and RD, were computed as in the following equations.

$$FA = \sqrt{\frac{3}{2}} \sqrt{\frac{(\lambda_1 - \bar{\lambda})^2 + (\lambda_2 - \bar{\lambda})^2 + (\lambda_3 - \bar{\lambda})^2}{\lambda_1^2 + \lambda_2^2 + \lambda_3^2}}$$

$$MD = \bar{\lambda} = (\lambda_1 + \lambda_2 + \lambda_3) / 3 = (AD + 2*RD) / 3$$

$$AD = \lambda_1$$

$$RD = (\lambda_2 + \lambda_3) / 2, \quad (1)$$

where λ_1 , λ_2 and λ_3 are the three eigenvalues of a diffusion tensor matrix in a descending order.

Spatial normalization

T1 image-based registration was used to warp the respective DTI images, instead of directly registering FA images or the low resolution T2 (*b* = 0) MR images. This was done since T1 images had a higher spatial resolution and signal-to-noise ratio when compared to DTI images and avoided possible biases resulting from a direct registration of FA images across subjects. Accordingly, the spatial normalization of DTI parametric maps involved the following three steps. *Preprocessing step*: Visual inspection of all images was performed to ensure no presence of bulk motion, and T1 images of each individual subject were segmented into white matter (WM), gray matter (GM) and CSF using the Markov Random Field based tissue segmentation approach provided in FSL 3.2 (Zhang et al., 2001). *Registration of T1 images across subjects*: The

HAMMER-based elastic registration (Shen and Davatzikos, 2002, 2003) approach was employed to align T1 images of all subjects (including both healthy controls and HIV+ patients) to a template, which is not a subject from this study and bears anatomical definitions of major brain structures (N. Kabani et al., 1998). One advantage of the HAMMER-based registration technique is that it uses sufficient geometrical attributes (calculated from multi-scale neighborhoods) to establish the image correspondence during the registration of the two images. *Registration of images within subject*: DTI images were rigidly aligned with the corresponding T1 images of each subject using a linear registration tool available in FSL 3.2 (Analysis Group, FMRIB, Oxford, UK). By completion of the above three steps, DTI parametric maps can be spatially normalized towards the template space.

Data analysis

ROI based analysis on mean DTI values for major white matter regions

In order to determine how white matter abnormalities are revealed by DTI across different brain white matter regions, a widely used digital atlas bearing anatomically parcellated white matter regions, including frontal, parietal, temporal and occipital white matter, corpus callosum, and internal capsule (Fig. 1) was chosen as the template (Kabani et al., 1998). For every subject, the mean values of FA, MD, AD and RD in each of these major white matter regions

were computed after mapping the digital atlas in the template space towards each individual subject through the transformation obtained from the image registration (discussed in the previous section).

Before comparing the mean DTI values from these ROIs between a patient group and the healthy control group, patients in both HND and HAD with and without HAART treatment were compared first using the Mann–Whitney U test to determine the potential drug related effects. Subsequently, for each DTI parameter in each white matter region, the Kruskal–Wallis statistical test was performed to test the validity of the null hypothesis that the three groups (NORMAL, HND and HAD) are equal. Pair-wised Mann–Whitney U tests were performed between every two groups when this null hypothesis was rejected with a small p value (e.g. $p < 0.05$).

Voxel-based group comparison

In order to identify the affected white matter regions at different cognitive impairment levels, group analysis was also conducted through a voxel-by-voxel comparison between each of the two HIV+ groups and the healthy controls. Before performing group comparison, all DTI images were spatially smoothed with an isotropic 3D Gaussian filter (6 mm in full width at half maximum (FWHM)) to remove noise and minimize the effects of inter-subject structural variations.

The voxel-based group comparison was performed in the following three steps (Zhu et al., 2007). The first step involved fitting a

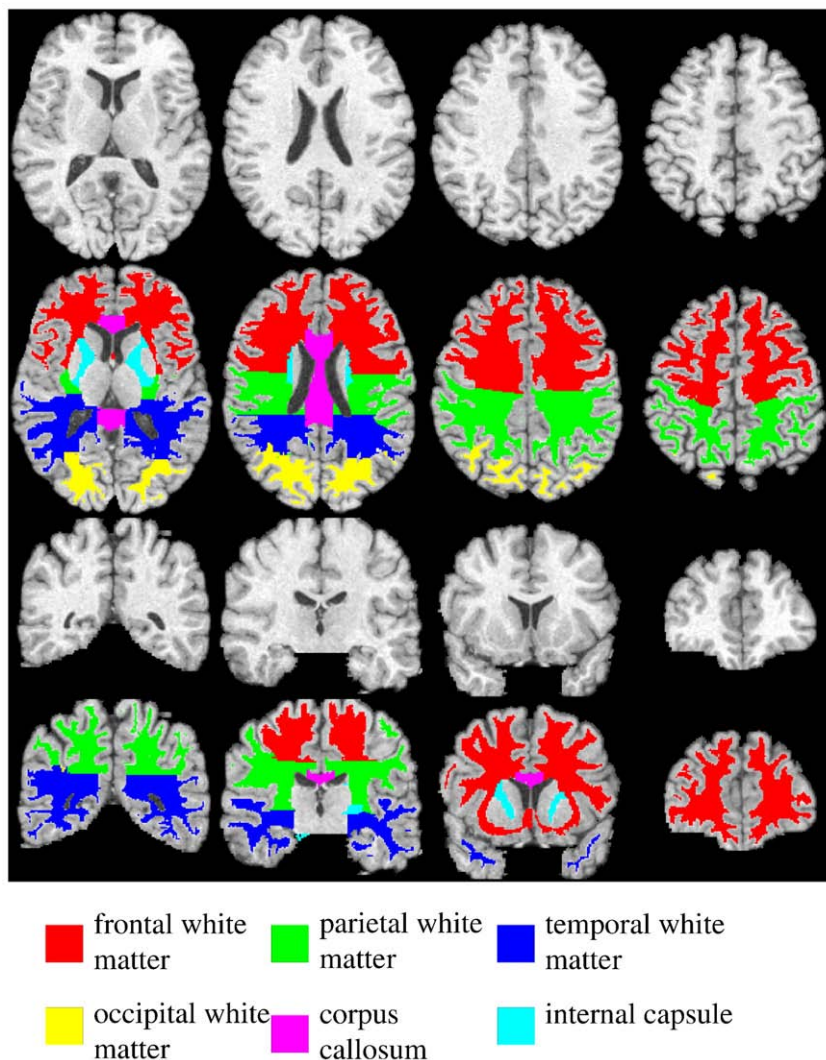


Fig. 1. Four axial (top two panels) and coronal (bottom two panels) slices of the template T1 images and the corresponding parcellated major white matter regions including frontal, parietal, temporal, occipital white matter, corpus callosum and internal capsule, respectively.

heteroscedastic linear model including diagnosis ($\text{NORMAL}(x_1)$, $\text{HND}(x_2)$, and $\text{HAD}(x_3)$) as the between-subject factor to a specific DTI parameter (e.g., FA) from all subjects (Eq. (2)).

$$y_t = \beta_1 * x_1 + \beta_2 * x_2 + \beta_3 * x_3 + \varepsilon_t = \vec{x}_t^T \vec{\beta} + \varepsilon_t, \quad (2)$$

Where, ε_t is the noise for subject t , and β_i ($i=1-3$) are coefficients for the generalized linear model. The heteroscedastic linear model was used here to avoid two key assumptions in the classical linear model: (1) the data conforms to a Gaussian distribution at each voxel, and (2) the variance of the imaging data is homogeneous across subjects. Thus, the heteroscedastic linear model is more suitable to a large class of distributions in the imaging data, such as the FA, since it may not conform to a Gaussian distribution. *The second step* was to test the hypothesis that whether two groups are significantly different from each other. The linear null hypothesis (Eq. (3)) was tested with a Wald-type statistic (Eq. (4)).

$$H_0 : R \vec{\beta} = b_0 \quad (3)$$

$$W_n = \left(R \vec{\beta} - b_0 \right)^T \Sigma^{-1} \left(R \vec{\beta} - b_0 \right) \quad (4)$$

Σ is a consistent estimate of the covariance matrix of $R \vec{\beta} - b_0$ under H_0 . For instance, in order to test whether NORMAL and HND were significantly different, the coefficients like $R = (1, -1, 0)$ and $b_0 = 0$ were chosen to determine whether the null hypothesis would be rejected with a small p value (e.g. $p < 0.05$). *The third step* was to calculate the adjusted p value to account for multiple statistical tests conducted across all voxels through controlling the family-wise error rate (Eq. (5)). This step is critical to control the type I error (false positive) given the large number of voxels involved in the comparison. The wild bootstrapping method also avoids the assumption of smoothness and Gaussian distribution for random field theory (as implemented in SPM).

$$p(d) \approx 1 / S \sum_{s=1}^S I(W_D^{*(s)} \geq W_n(d)) \quad (5)$$

$W_D^{*(s)}$ is the maximum of the Wald statistics within the whole region D at the s th step of the wild bootstrapping (total S steps), and I is a binary indicator function. The final significant regions will be defined as the voxels with the adjusted p value less than 0.05.

As in the previous ROI based analysis, HAART administration was also assessed as the between-subject factor and the similar process was applied to examine whether significantly different brain regions associated with medication use exist. After no significance was found for medication use, patients within the same cognitive impairment level (HND or HAD) were pooled together for a comparison with the healthy control.

Results

Evaluation of drug therapeutic effect

In both HND and HAD groups, no significant difference was found between patients with and without HAART in the above analyses. It might suggest either that HAART had no substantial effect on DTI values, or that the effects of this antiretroviral therapy could not be adequately discerned in this cross-sectional study due to either the insufficient number of patients in each patient group or the limitations of the current experimental setting. Nevertheless, it remains controversial as to how effective HAART is in improving cognitive function (Chang et al., 1999; Dore et al., 1999; Gray et al., 2003).

Spatial normalization

After registration, the mean and standard deviation maps of the warped four DTI parameters from all 47 subjects are provided in Fig. 2. The effectiveness of the spatial normalization is qualitatively demonstrated in the mean (panels A1 to D1, Fig. 2) and standard deviation (panels A2 to D2, Fig. 2) images of all four DTI parameters. In the mean FA image (panel A1, Fig. 2), detailed white matter structures including the white matter tracts within the cortical areas are clearly visible without being blurred by inaccuracy in registration. In the mean MD image (panel B1, Fig. 2), the contrast between gray and white matter is not as strong as that in the mean FA image due to the more homogeneous nature of MD across the brain. AD is higher in major white matters (panel C1, Fig. 2) while RD is lower in such areas (panel D1, Fig. 2). Furthermore, the corresponding standard deviation images (panels A2 to D2, Fig. 2) of these four DTI parameters from all 47 subjects are low when compared to the corresponding mean images. These results demonstrate the quality of the employed registration method.

Statistical comparison of mean DTI values from major white matter areas

Fig. 3 summarizes the significant findings in four diffusion parameters at different brain regions for HND and HAD groups. We

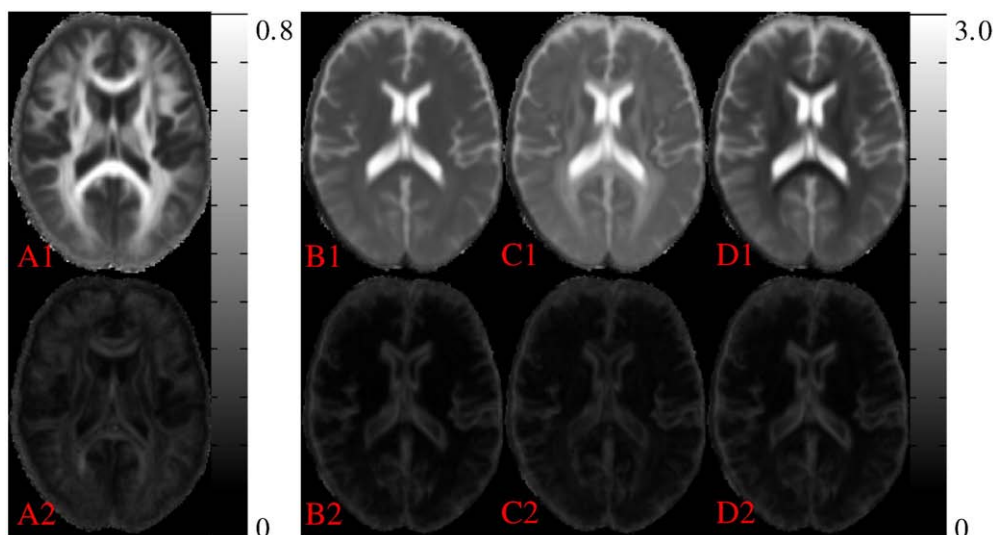


Fig. 2. The mean (top panel) and standard deviation (bottom panel) maps of FA, MD, AD and RD ($10^{-3} \text{ mm}^2/\text{s}$ for diffusivities) from all 47 subjects. For each DTI parameter, cross-sectional views of the mean and standard deviation maps are displayed with the same contrast to demonstrate the relative signal strength between them.

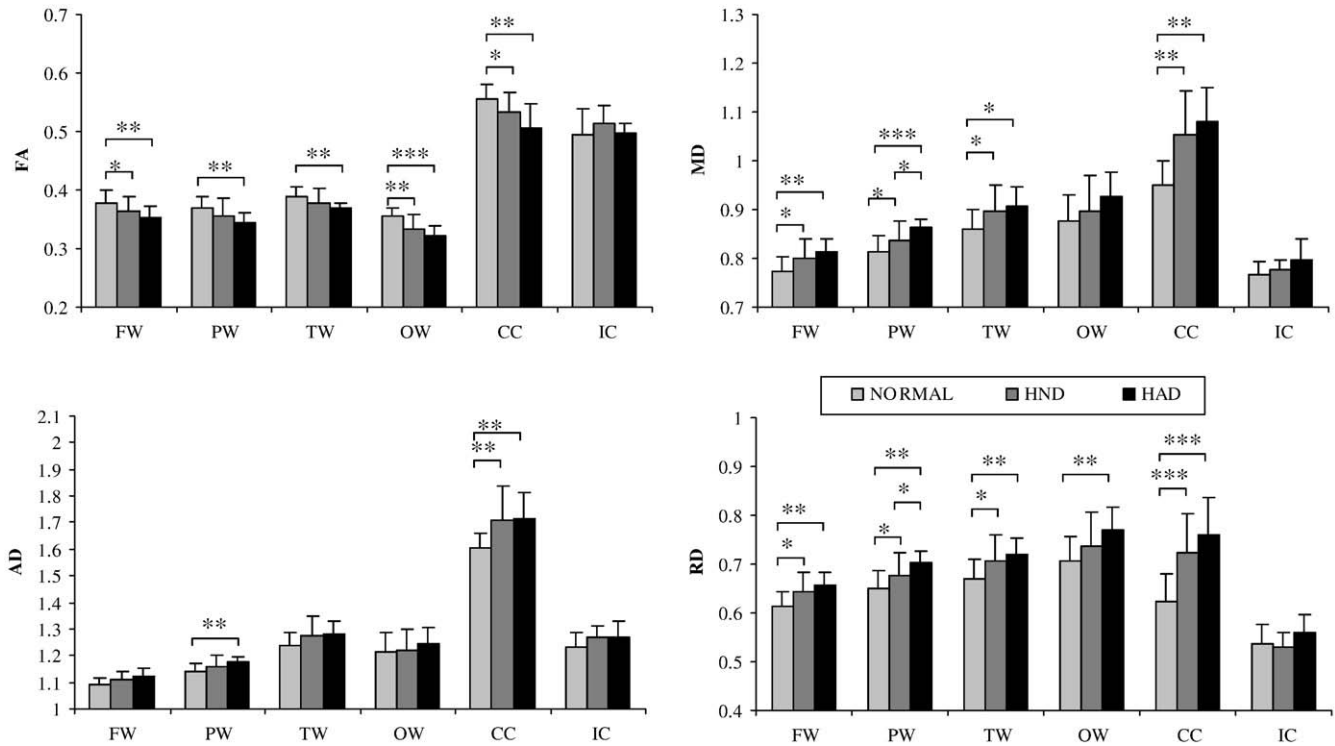


Fig. 3. The mean and standard deviation of the mean DTI parameters (FA, MD, AD and RD) for NORMAL, HND and HAD within frontal (FW), parietal (PW), temporal (TW) and occipital (OW) white matter, corpus callosum (CC) and internal capsule (IC). Symbols *, ** and *** indicate the statistical significant level of $p < 0.05$, $p < 0.01$ and $p < 0.001$, respectively.

found that the major abnormalities manifested in these four DTI parameters caused by HIV infection are a decrease in FA and increases in MD, AD and RD. In FA, HAD demonstrated significant decrease in frontal ($p < 0.01$), parietal ($p < 0.01$), temporal ($p < 0.01$), occipital ($p < 0.001$) white matter and corpus callosum ($p < 0.01$), while HND only demonstrated significant decrease in frontal ($p < 0.05$), occipital ($p < 0.01$) white matter and corpus callosum ($p < 0.01$). In MD, both HAD and HND demonstrated a significant increase in frontal ($p < 0.05$ for HND and $p < 0.01$ for HAD), parietal ($p < 0.05$ for HND and $p < 0.001$ for HAD), temporal ($p < 0.05$ for both) white matter and corpus callosum ($p < 0.01$ for both). In addition, significant difference between HAD and HND was observed in parietal white matter ($p < 0.05$). The differences in AD among groups were qualitatively less remarkable when compared to the remaining three diffusion measures; a significant increase of AD was observed in parietal white matter ($p < 0.01$) and corpus callosum ($p < 0.01$) in HAD, while HND only demonstrated significant increase in corpus callosum ($p < 0.01$). Finally, HAD patients demonstrated a significant increase in RD in frontal ($p < 0.01$), parietal ($p < 0.01$), temporal ($p < 0.01$), occipital ($p < 0.01$) white matter and corpus callosum ($p < 0.001$), while HND patients demonstrated a significant increase in frontal ($p < 0.05$), parietal ($p < 0.05$), temporal ($p < 0.05$) white matter and corpus callosum ($p < 0.001$). In addition, a significant difference between HND and HAD was detected within parietal white matter ($p < 0.05$). Interestingly, no differences were observed in the internal capsule for all four diffusion parameters among the three groups.

Voxel-based group comparison

Compared to the healthy control group, diffuse abnormal brain regions with significantly reduced FA or significantly elevated MD, AD, and RD were identified in both HND and HAD patients. Abnormal brain regions identified in HND and HAD illustrated in ten uniformly separated axial slices in Fig. 4. In both HND and HAD patients, brain abnormality was found in all major white matter regions, including the frontal white matter (FW), parietal white matter (PW), temporal

white matter (TW), occipital white matter (OW), corona radiata (CR), corpus callosum (CC), optic radiation (OR), and external capsule (EC) with these four DTI parameters. The total volumes of the identified abnormal regions in different brain lobes are summarized in Fig. 5. In both HND and HAD, the identified abnormal regions were primarily distributed in frontal, parietal and temporal white matter regions than other white matter areas (Fig. 5). The HAD patient group consistently had a higher volume of abnormal white matter than HND in all these white matter regions and in all four DTI parameters (Fig. 5). Voxel-based analysis also revealed that HIV infection affected these four DTI parameters to a different extent, so the analysis based upon a single DTI parameter or even FA and MD jointly may not be sufficient for a comprehensive analysis of white matter abnormality caused by HIV infection. Interestingly, more abnormal regions were identified with RD than AD, which was demonstrated as the much higher volumes in all white matter regions in RD (Fig. 5). This finding agrees with the ROI based results and also suggests that HIV infection affects RD to a greater extent than AD.

Discussion

In this study, both ROI based and voxel-based comparisons of DTI among normal control subjects, HAD, and HND support the following major findings: 1) HIV infection causes wide spread abnormalities in different white matter regions, 2) the white matter alteration in HAD is more severe than HND, suggesting the potential of a DTI based white matter radiological feature to distinguish HAD from HND and 3) HIV infection affects RD to a greater extent than AD, which may suggest that alteration of RD may reflect the prominent disease process in both HND and HAD.

Evaluation of white matter abnormalities in different geometrical scales

In our study, both the ROI and voxel-based analysis approaches were employed to discern the potential white matter abnormalities in HAD and HND patients owing to the fact that these two methods are

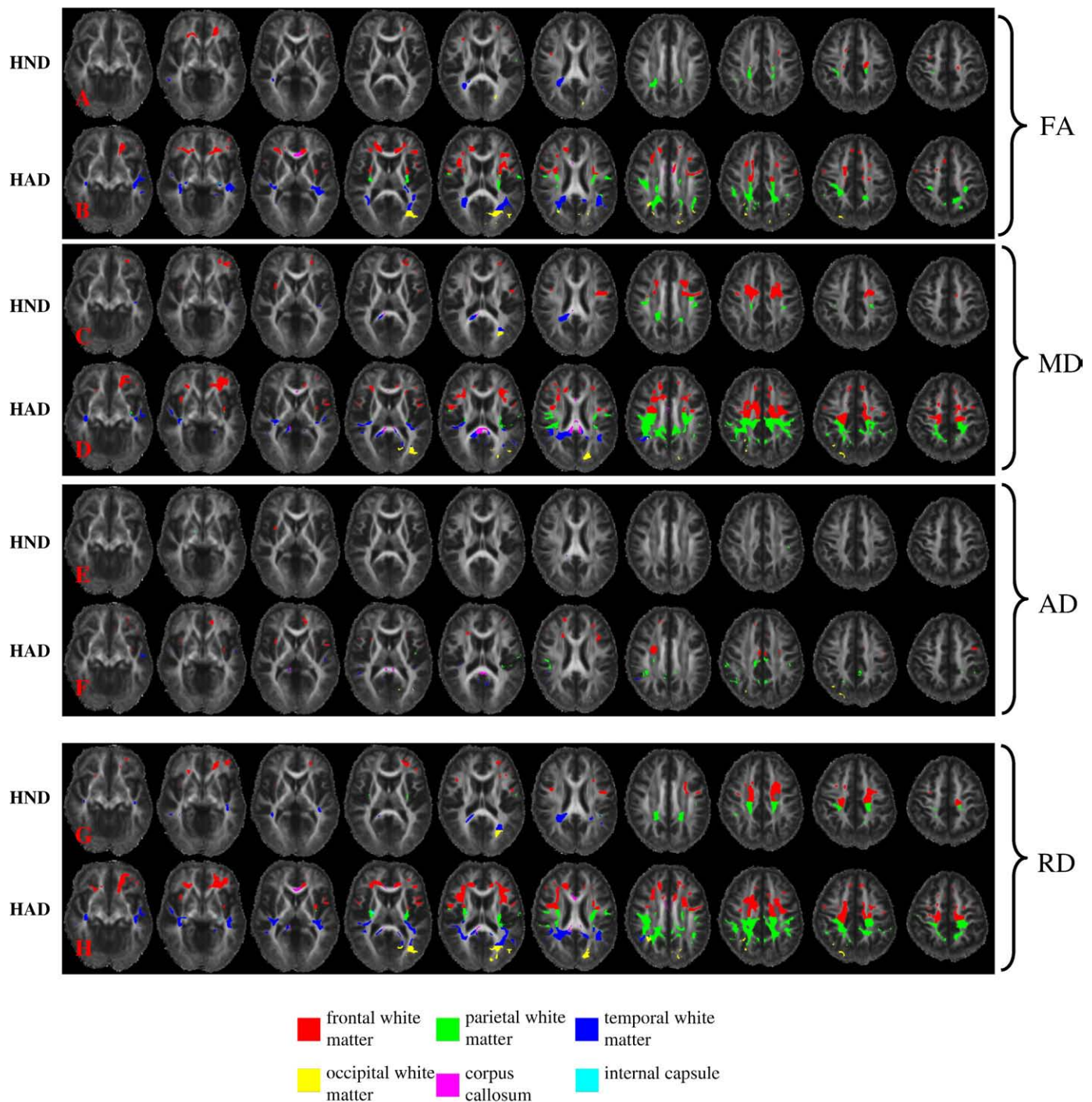


Fig. 4. The abnormal white matter regions detected in HND and HAD patient groups with voxel-based analysis in FA, MD, AD and RD. The affected brain areas with significantly reduced FA and elevated MD, AD, and RD in HND and HAD patient groups are superimposed upon the mean FA map of the healthy controls.

associated with different geometrical scales and complementary to each other. The regional based analysis performs statistical comparisons in a larger geometrical scale, and it is a global measure of abnormality for a particular predefined white matter region. Although this approach cannot delineate the affected regions at a voxel level, it is less sensitive to potential registration inaccuracy and has a high statistical power. In contrast, the automatic data-driven voxel-based analysis is able to delineate detailed abnormal brain regions. Nevertheless, the sensitivity of voxel-based analysis may be dampened by 1) the need to adjust for multiple comparisons associated with the large number of voxels and 2) when there is a lack of consistent regions of

the brain abnormality in HIV patients. Thus, these two approaches were used jointly in our study for a more comprehensive analysis of the impact of HIV infection on white matter.

Identified white matter abnormalities in comparison to previous HIV studies

In general, the identified white matter abnormalities in our study agree with previous HIV studies, although a thorough comparison with the previous findings is formidable due to the differences in patient populations, experimental designs and the employed analyzing methods. The abnormalities of frontal white matter, corpus callosum,

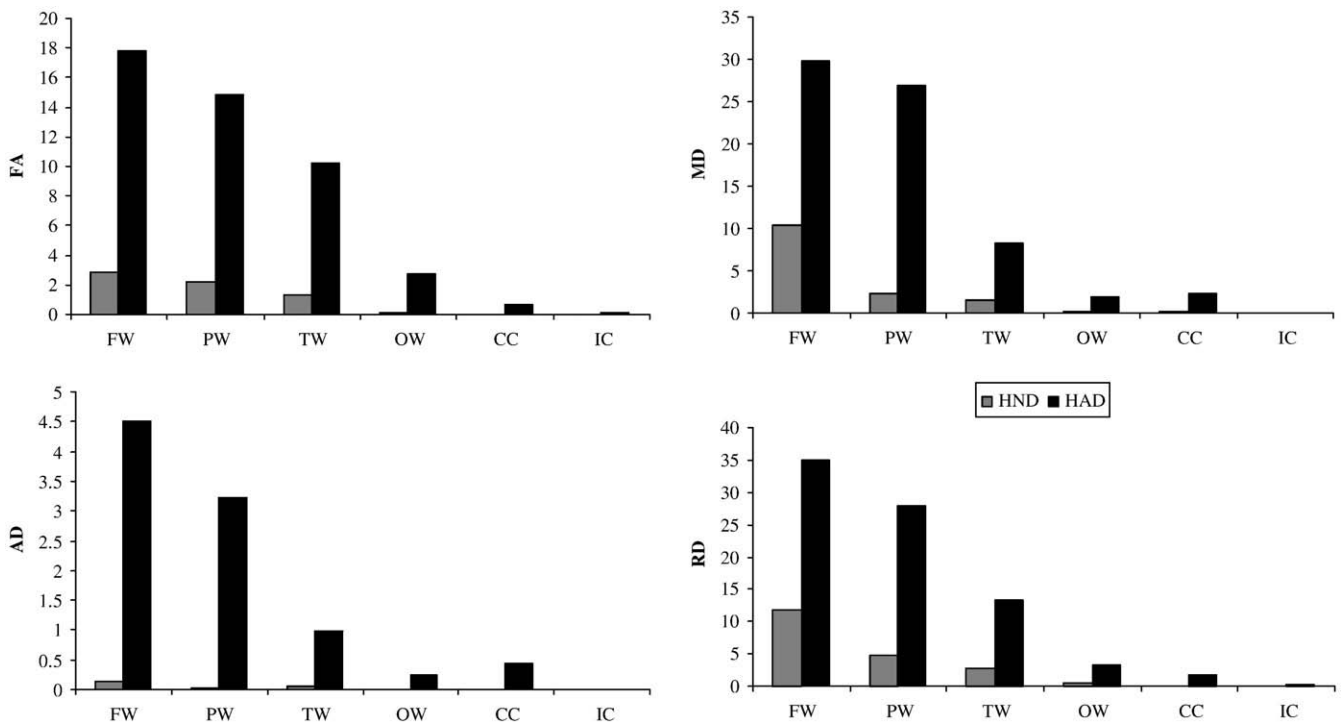


Fig. 5. The total volume of the identified significant regions by voxel-based analysis (cm^3) with FA, MD, AD and RD, for HND and HAD patients in different major white matter regions.

internal capsule and corona radiata have been reported previously with ROI based HIV studies with DTI. In the ROI based study by Pomara et al. (2001), frontal lobes and posterior limbs of internal capsule were identified as abnormal with FA, but no statistical significance was detected in corpus callosum, temporal lobe and parietal lobe. In ADC, no statistical significance was detected in any regions in this study (Pomara et al., 2001). In the work by Thurnher et al. (2005), significant decrease in FA was only found in the genu of corpus callosum in 60 HIV+ patients. Interestingly, in another ROI based study by Wu et al. (2006), significant increase in MD and significant decrease in FA were only detected in splenium and not in genu and frontal white matter. Thus, even for ROI based analysis, these studies do not have consistent findings regarding to the identified abnormal brain regions. In our study, we have identified splenium having a significant increase in MD in HND and HAD patients and genu has a significant decrease in FA in HAD patients (panel B, Fig. 4). Our global ROI based analysis also demonstrated significant changes in all four DTI parameters in corpus callosum for both HND and HAD patients. For the internal capsule, we found regions in posterior limb having increased MD in HAD patients (panel D, Fig. 4), we did not find significant regions with increased FA as demonstrated by Pomara et al. (2001). We have demonstrated the involvement of corona radiata in both HND (panel C, Fig. 4) and HAD (panel D, Fig. 4) patients with MD. In another study by Ragin et al. (2005), the MD value at semiovale (a part of corona radiata) was significantly correlated with visual memory deficits and visuocognition. Besides the abnormalities in frontal white matter, corpus callosum, internal capsule and corona radiata, we have also identified abnormalities located in occipital white matter (including optic radiata) in both voxel-based (the yellow regions in panels B, D, and H, Fig. 4) and global ROI-based (Fig. 3) comparisons. To our best knowledge, this result has not been reported previously in DTI based HIV studies. But there exists autopsy evidence from HIV+ patients who died of unnatural courses (e.g. drug overdose and body gunshot) (Gray et al., 1992). In this autopsy study, abnormal white matter pallor in corpus callosum, optic radiata and internal capsule were only found in HIV+ subjects but not in the negative controls with matched causes of death.

Different alterations in axial and radial diffusivities caused by HIV infection

Both the ROI based and voxel-based comparisons consistently support that the increase in RD is more significant than the increase in AD in both HND and HAD patients. The ROI based analysis demonstrated more white matter regions having significantly altered RD than AD (Fig. 3), and the voxel-based analysis revealed a larger volume in the identified significant regions with RD than AD (Fig. 5). These results strongly support that the alteration in these two diffusivities is different. Previous shiverer and cuprizone mouse studies suggested that changes in AD and RD might be associated with axonal and myelin injuries, respectively (Song et al., 2002; Sun et al., 2006). Thus, our results suggest that demyelination as reflected by the increase in RD may be the prominent disease process associated with HIV infection in both HND and HAD, and axonal injury may occur at a weaker level.

Although whether or not AD can truthfully reveal axonal injury in white matter remains an ongoing investigation, the presence of axonal injury has been discovered by previous immuno-histochemical studies using β -amyloid precursor protein (β -APP) – a marker for axonal injury (An and Scaravilli, 1997; Giometto et al., 1997; Gray et al., 1998; Medana and Esiri, 2003; Raja et al., 1997). In our study, significant alterations of AD were observed in multiple white matter regions, and our results suggested that alteration of AD was more severe in HAD than HND. The ROI based analysis revealed that corpus callosum had a significant increase in AD in both HND and HAD patients, and parietal white matter had a significant increase in HAD only (Fig. 3). All of the remaining white matter regions for both HND and HAD only demonstrated an increasing trend (increased mean AD value) when compared with the healthy controls. HAD demonstrated several abnormal regions located in frontal white matter, parietal white matter, corpus callosum and external capsule (panel F, Fig. 4) using the voxel-based analysis while only a small region in the external capsule was identified for HND (panel E, Fig. 4). The total volume of the identified significant regions was also greater in HAD than HND (Fig. 5).

Compared to AD, RD may be a more truthful reflector of myelin abnormality. The reported white matter abnormalities identified with RD in this study agree with previous literatures. Histopathologic studies have demonstrated that myelin injury is a prominent component of white matter injury. In autopsy studies, diffuse white matter damage in HIV+ patients appears as pallor in sections stained for myelin damage (Price et al., 1988; Raja et al., 1997). Furthermore, Gray et al. (1996) found that myelin pallor and subsequent gliosis occurred even at the asymptomatic stage. In an early study measuring myelin basic protein in CSF of HIV+ patients, an increased myelin basic protein level in CSF was detected in all patients with severe dementia (100%), while only 28% and 44% of the patients with mild and moderate dementia were found with increased myelin basic protein in CSF. No myelin basic protein was found in HIV+ patients without neurological disorders or in seronegative, healthy controls. This CSF study suggests that the degree of myelin abnormalities may correlate with functional status in patients with neurological disorders (Liuzzi et al., 1992). Our results of increased white matter abnormality observed with RD in both HND and HAD seemingly agree with this CSF study (Liuzzi et al., 1992).

Elevated white matter alteration in HAD compared to HND

In the past, there were several white matter related studies examining the correlation between cognitive impairment and imaging results (including FA or MD and volume loss computed with T1 anatomical image) (Ragin et al., 2004b, 2005; Cloak et al., 2004; Chiang et al., 2007). These studies used a mixed subject population including both healthy control and HIV+ patients, and were more focused on revealing brain abnormality caused by HIV infection rather than comparing the imaging findings among HIV+ patients with different levels of cognitive impairment. Different from these published studies, our study employed a direct pairwise comparison among NORMAL, HND and HAD. Our results revealed a more prominent white matter alteration in HAD compared to HND (Figs. 3–5), and importantly, this finding is consistent with both ROI based and voxel-based analysis.

Previous studies have revealed that HAD has significantly higher atrophies in cerebral gray matter and basal ganglia (Aylward et al., 1995, 1993). Our work may be the first one to investigate the existence of white matter difference between HND and HAD. Our study revealed that statistically significant differences existed between HAD and HND patients in parietal white matter, suggesting that this abnormality may be related to stages of disease. Moreover, HAD exhibited dramatically larger abnormal areas in the posterior part of frontal white matter and anterior part of parietal white matter (red and green areas in panels C, D, G, H, Fig. 4) with voxel-based analysis. Interestingly, these regions are projected towards the sensorimotor cortex. The similar region has been identified by Ragin et al. (2005) in a correlation study with visual memory deficits and visuconstruction. In addition, white matter volume loss has been observed in the primary and association sensorimotor areas in HIV+ patients (Chiang et al., 2007). In consistency with these published works, our results may suggest that demyelination at these regions (especially in parietal white matter) may be correlated with the worsening of cognitive impairment in HAD.

Technical considerations

DTI is a versatile imaging technique where many diffusion related measures can be derived from the scalar and vector components of the diffusion tensor matrix. In this study, we focused upon four DTI parameters to discern potential white matter abnormalities in HIV+ patients, namely FA, MD, AD and RD. The choice of FA and MD mainly reflects the popularity of both parameters in the literature utilizing DTI to discern white matter abnormalities. While both FA and MD have been widely utilized, their inability to potentially provide insights into the biological underpinnings associated with the abnormal white

matter has been implicated by Song et al. (2002). Therefore, to circumvent this limitation associated with FA and MD, AD and RD were chosen to delineate potential axonal injury and demyelination in HIV+ patients in our studies. Nevertheless, other DTI parameters could also be considered to identify white matter abnormalities, including volume ratio ($VR = \lambda_1 * \lambda_2 * \lambda_3 / \bar{\lambda}^3$) (Sundgren et al., 2004), relative anisotropy ($RA = \sqrt{((\lambda_1 - \bar{\lambda})^2 + (\lambda_2 - \bar{\lambda})^2 + (\lambda_3 - \bar{\lambda})^2)} / \sqrt{3\bar{\lambda}}$) (Sundgren et al., 2004), linear component ($lc = (\lambda_1 - \lambda_2) / \lambda_1$), planar component ($pc = (\lambda_2 - \lambda_3) / \lambda_1$), spherical component ($sc = \lambda_3 / \lambda_1$) (Westin et al., 2002) or major eigenvector (corresponding to the largest eigenvalue). Although these parameters were not specifically investigated in our studies, the proposed voxel-based group analysis approaches can be directly applied to other diffusion parameters.

In this paper, the registration of T1 and DTI image was achieved by a linear registration algorithm. To further improve their alignment, B0 image of DTI can be registered with T1 using a non-linear registration algorithm to compensate the geometrical distortion presented in DTI images. It is worth noting that although there may exist slight inaccuracy in the linear registration between T1 and DTI images, the smoothing operation prior to the voxel-based statistical comparison makes our whole analysis process robust to this possible slight misalignment due to the distortion of DTI.

Conclusion

Our initial experience with analyzing brain abnormality in HND and HAD patients with multiple DTI parameters is promising. Our results support that HIV infection causes widespread abnormalities in different white matter regions in both HND and HAD patients and white matter alteration is more severe in HAD than HND patients. Furthermore, we have found that the dominance of alteration in RD compared to AD may reflect the prominent disease progression associated with white matter demyelination.

References

- AIDSTaskForce, 1991. Nomenclature and research case definitions for neurologic manifestations of human immunodeficiency virus-type 1 (HIV-1) infection. Report of a Working Group of the American Academy of Neurology AIDS Task Force. *Neurology* 41, 778–785.
- Albright, A.V., Soldan, S.S., Gonzalez-Scarano, F., 2003. Pathogenesis of human immunodeficiency virus-induced neurological disease. *J. Neurovirol.* 9, 222–227.
- An, S.F., Scaravilli, F., 1997. Early HIV-1 infection of the central nervous system. *Arch. Anat. Cytol. Pathol.* 45, 94–105.
- Aylward, E.H., Brettschneider, P.D., McArthur, J.C., Harris, G.J., Schlaepfer, T.E., Henderer, J.D., Barta, P.E., Tien, A.Y., Pearlson, G.D., 1995. Magnetic resonance imaging measurement of gray matter volume reductions in HIV dementia. *Am. J. Psychiatry* 152, 987–994.
- Aylward, E.H., Henderer, J.D., McArthur, J.C., Brettschneider, P.D., Harris, G.J., Barta, P.E., Pearlson, G.D., 1993. Reduced basal ganglia volume in HIV-1-associated dementia: results from quantitative neuroimaging. *Neurology* 43, 2099–2104.
- Basser, P.J., Mattiello, J., LeBihan, D., 1994. Estimation of the effective self-diffusion tensor from the NMR spin echo. *J. Magn. Reson., Ser. B* 103, 247–254.
- Chang, L., Ernst, T., Leonido-Yee, M., Witt, M., Speck, O., Walot, I., Miller, E.N., 1999. Highly active antiretroviral therapy reverses brain metabolite abnormalities in mild HIV dementia. *Neurology* 53, 782–789.
- Chiang, M.C., Dutton, R.A., Hayashi, K.M., Lopez, O.L., Aizenstein, H.J., Toga, A.W., Becker, J.T., Thompson, P.M., 2007. 3D pattern of brain atrophy in HIV/AIDS visualized using tensor-based morphometry. *Neuroimage* 34, 44–60.
- Cloak, C.C., Chang, L., Ernst, T., 2004. Increased frontal white matter diffusion is associated with glial metabolites and psychomotor slowing in HIV. *J. Neuroimmunol.* 157, 147–152.
- Dore, G.J., Correll, P.K., Li, Y., Kaldor, J.M., Cooper, D.A., Brew, B.J., 1999. Changes to AIDS dementia complex in the era of highly active antiretroviral therapy. *Aids* 13, 1249–1253.
- Filippi, C.G., Ulug, A.M., Ryan, E., Ferrando, S.J., van Gorp, W., 2001. Diffusion tensor imaging of patients with HIV and normal-appearing white matter on MR images of the brain. [see comment]. *Ajnr: Am. J. Neuroradiol.* 22, 277–283.
- Giometto, B., An, S.F., Groves, M., Scaravilli, T., Geddes, J.F., Miller, R., Tavolato, B., Beckett, A.A., Scaravilli, F., 1997. Accumulation of beta-amyloid precursor protein in HIV encephalitis: relationship with neuropsychological abnormalities. *Ann. Neurol.* 42, 34–40.
- Gonzalez-Scarano, F., Martin-Garcia, J., 2005. The neuropathogenesis of AIDS. *Nat. Rev. Immunol.* 5, 69–81.

- Gray, F., Belec, L., Chretien, F., Dubreuil-Lemaire, M.L., Ricolfi, F., Wingertsmann, L., Poron, F., Gherardi, R., 1998. Acute, relapsing brain oedema with diffuse blood-brain barrier alteration and axonal damage in the acquired immunodeficiency syndrome. *Neuropathol. Appl. Neurobiol.* 24, 209–216.
- Gray, F., Chretien, F., Vallat-Decouvelaere, A.V., Scaravilli, F., 2003. The changing pattern of HIV neuropathology in the HAART era. *J. Neuropathol. Exp. Neurol.* 62, 429–440.
- Gray, F., Lesca, M.C., Keohane, C., Paraire, F., Marc, B., Durigon, M., Gherardi, R., 1992. Early brain changes in HIV infection: neuropathological study of 11 HIV seropositive, non-AIDS cases. *J. Neuropathol. Exp. Neurol.* 51, 177–185.
- Gray, F., Scaravilli, F., Everall, I., Chretien, F., An, S., Boche, D., Adle-Biassette, H., Wingertsmann, L., Durigon, M., Hurtrel, B., Chiodi, F., Bell, J., Lantos, P., 1996. Neuropathology of early HIV-1 infection. *Brain Pathol.* 6, 1–15.
- Kabani, N., J.D.M., Holmes, C.J., Evans, A.C., 1998. A 3D atlas of the human brain. *Neuroimage* 7, S717.
- Kraus, M.F., Susmaras, T., Caughlin, B.P., Walker, C.J., Sweeney, J.A., Little, D.M., 2007. White matter integrity and cognition in chronic traumatic brain injury: a diffusion tensor imaging study. *Brain* 130, 2508–2519.
- Langford, T.D., Letendre, S.L., Larrea, G.J., Masliah, E., 2003. Changing patterns in the neuropathogenesis of HIV during the HAART era. *Brain Pathol.* 13, 195–210.
- Liuzzi, G.M., Mastroianni, C.M., Vullo, V., Jirillo, E., Delia, S., Riccio, P., 1992. Cerebrospinal fluid myelin basic protein as predictive marker of demyelination in AIDS dementia complex. *J. Neuroimmunol.* 36, 251–254.
- Masliah, E., DeTeresa, R.M., Mallory, M.E., Hansen, L.A., 2000. Changes in pathological findings at autopsy in AIDS cases for the last 15 years. *Aids* 14, 69–74.
- McArthur, J.C., Hoover, D.R., Bacellar, H., Miller, E.N., Cohen, B.A., Becker, J.T., Graham, N.M., McArthur, J.H., Selnes, O.A., Jacobson, L.P., et al., 1993. Dementia in AIDS patients: incidence and risk factors. Multicenter AIDS Cohort Study. *Neurology* 43, 2245–2252.
- Medana, I.M., Esiri, M.M., 2003. Axonal damage: a key predictor of outcome in human CNS diseases. *Brain* 126, 515–530.
- Moroni, M., Antinori, S., 2003. HIV and direct damage of organs: disease spectrum before and during the highly active antiretroviral therapy era. *Aids* 17 (Suppl 1), S51–64.
- Pomara, N., Crandall, D.T., Choi, S.J., Johnson, G., Lim, K.O., 2001. White matter abnormalities in HIV-1 infection: a diffusion tensor imaging study. *Psychiatry Res.* 106, 15–24.
- Price, R.W., Brew, B., Sidtis, J., Rosenblum, M., Scheck, A.C., Cleary, P., 1988. The brain in AIDS: central nervous system HIV-1 infection and AIDS dementia complex. *Science* 239, 586–592.
- Ragin, A.B., Storey, P., Cohen, B.A., Edelman, R.R., Epstein, L.G., 2004a. Disease burden in HIV-associated cognitive impairment: a study of whole-brain imaging measures. *Neurology* 63, 2293–2297.
- Ragin, A.B., Storey, P., Cohen, B.A., Epstein, L.G., Edelman, R.R., 2004b. Whole brain diffusion tensor imaging in HIV-associated cognitive impairment. *AJNR Am. J. Neuroradiol.* 25, 195–200.
- Ragin, A.B., Wu, Y., Storey, P., Cohen, B.A., Edelman, R.R., Epstein, L.G., 2005. Diffusion tensor imaging of subcortical brain injury in patients infected with human immunodeficiency virus. *J. Neurovirol.* 11, 292–298.
- Raja, F., Sherriff, F.E., Morris, C.S., Bridges, L.R., Esiri, M.M., 1997. Cerebral white matter damage in HIV infection demonstrated using beta-amyloid precursor protein immunoreactivity. *Acta Neuropathol. (Berl)* 93, 184–189.
- Shen, D., Davatzikos, C., 2002. HAMMER: hierarchical attribute matching mechanism for elastic registration. *IEEE Trans. Med. Imaging* 21, 1421–1439.
- Shen, D., Davatzikos, C., 2003. Very high-resolution morphometry using mass-preserving deformations and HAMMER elastic registration. *Neuroimage* 18, 28–41.
- Song, S.K., Sun, S.W., Ramsbottom, M.J., Chang, C., Russell, J., Cross, A.H., 2002. Demyelination revealed through MRI as increased radial (but unchanged axial) diffusion of water. *Neuroimage* 17, 1429–1436.
- Stebbins, G.T., Smith, C.A., Bartt, R.E., Kessler, H.A., Adeyemi, O.M., Martin, E., Cox, J.L., Bammer, R., Moseley, M.E., 2007. HIV-associated alterations in normal-appearing white matter: a voxel-wise diffusion tensor imaging study. *J. Acquir. Immune. Defic. Syndr.* 46, 564–573.
- Sun, S.W., Liang, H.F., Trinkaus, K., Cross, A.H., Armstrong, R.C., Song, S.K., 2006. Noninvasive detection of cuprizone induced axonal damage and demyelination in the mouse corpus callosum. *Magn. Reson. Med.* 55, 302–308.
- Sundgren, P.C., Dong, Q., Gomez-Hassan, D., Mukherji, S.K., Maly, P., Welsh, R., 2004. Diffusion tensor imaging of the brain: review of clinical applications. *Neuroradiology* 46, 339–350.
- Thurnher, M.M., Castillo, M., Stadler, A., Rieger, A., Schmid, B., Sundgren, P.C., 2005. Diffusion-tensor MR imaging of the brain in human immunodeficiency virus-positive patients. *AJNR Am. J. Neuroradiol.* 26, 2275–2281.
- Westin, C.F., Maier, S.E., Mamata, H., Nabavi, A., Jolesz, F.A., Kikinis, R., 2002. Processing and visualization for diffusion tensor MRI. *Med. Image. Anal.* 6, 93–108.
- Wu, Y., Storey, P., Cohen, B.A., Epstein, L.G., Edelman, R.R., Ragin, A.B., 2006. Diffusion alterations in corpus callosum of patients with HIV. *AJNR Am. J. Neuroradiol.* 27, 656–660.
- Zhang, Y., Brady, M., Smith, S., 2001. Segmentation of brain MR images through a hidden Markov random field model and the expectation-maximization algorithm. *IEEE Trans. Med. Imaging* 20, 45–57.
- Zhu, H., JG, I., NS, T., R, D., X, H., R, B., Peterson, B.S., 2007. A statistical analysis of brain morphology using wild bootstrapping. *IEEE Trans. Med. Imaging* 26, 954–966.